Electronic Supplementary Information

Giant barocaloric effect with wide refrigeration temperature range in ethylene vinyl acetate copolymer

Chengliang Zhang,* Dunhui Wang,* Suxin Qian, Zhengming Zhang, Xiaohui Liang, Liqian Wu, Liyuan Long, Haifeng Shi and Zhida Han

Contents

1. Materials

The low-density PE was supplied by Shenhua Group, China (LDPE 2426H). The EVA copolymers, which contain 18%, 28% and 40% VA by weight with the nominal densities of 0.937, 0.951 and 0.965 g cm^{-3}, the nominal melting/freezing points of 346/326 K, 333/312 K and 320/300 K, and the nominal melt flow rate (at 463 K) of 150, 400 and 52 g 10 min^{-1}, were supplied by Dow Inc. (Elvax TM, 420, 210W, and 40W, respectively).

2. General features

2.1 Fourier transform infrared (FT-IR) spectroscopies

FT-IR were performed at RT using Nicolet 5700 (Thermo Electron, USA) for tablets samples (thickness~1mm) prepared by hot-pressing at about 400 K for 60 s under 5 MPa to check the chemical constitutions of the purchased PE and EVA samples (Fig. S1). The peaks at 2920 and 2852 cm^{-1} are due to the -CH_2- stretching vibrations,[1] while the peak at 1463 cm^{-1} is related to the -CH_2- deformation vibration.[1-2] As for the peak at 720 cm^{-1}, it is assigned to the -CH_2-CH_2-CH_2- sequences.[3] Compared with the PE, the EVAs exhibit additional peaks of the C=O stretching (1737 cm^{-1}),[1-2] and the -C-O-C- stretching vibrations (1240 and 1020 cm^{-1}),[2,4] due to the existence of the polar -$CH(OCOCH_3)$- comonomer. The peak at 1370 cm^{-1} reveals -CH_3 groups, which is originated either from alkyl branches or chain-end groups.[2]

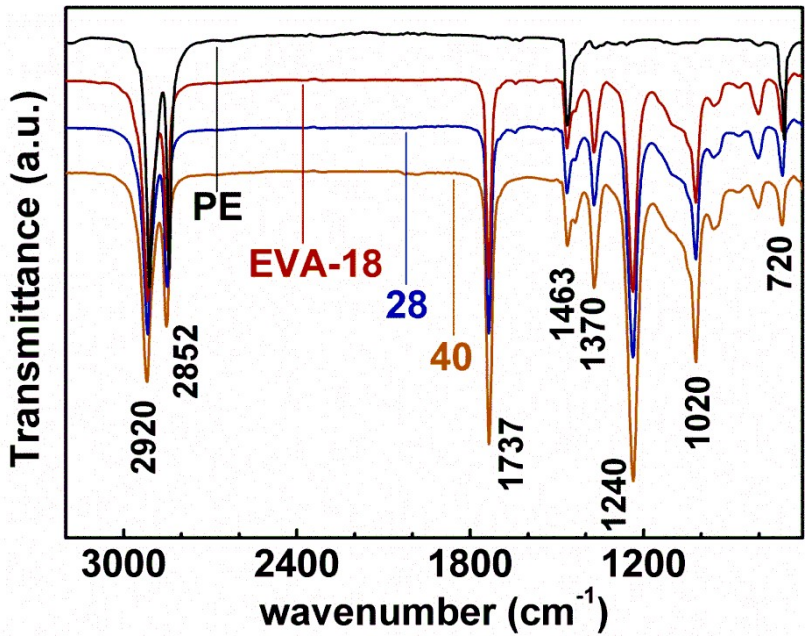

Fig. S1. FT-IR spectrums measured at RT for the PE and EVAs.

2.2 X-ray diffraction (XRD) patterns

The crystal structures of the PE and EVAs are characterized by XRD with Cu-Kα radiation at RT (Fig. S2). It is found that the PE has an orthorhombic structure at ambient pressure.[5] But in the case of the EVAs, they are dominated by the amorphous states, which can be ascribed to the decreased chains regularities by introducing VA-groups.[6-7]

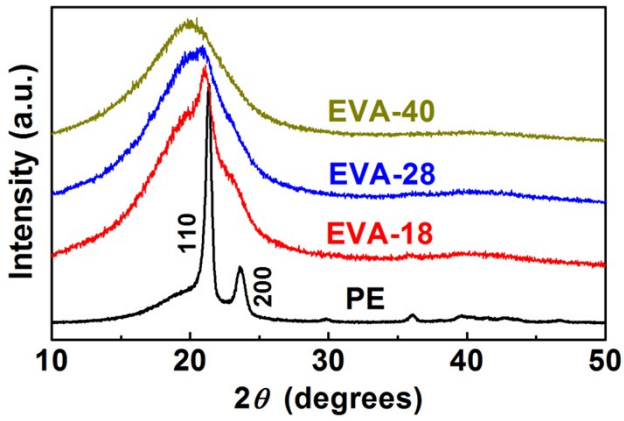

Fig. S2. XRD patterns measured at RT for the PE and EVAs.

2.3 Typical liquid and solid states of EVA

The EVA-18 is taken as an example to show the solid and liquid states of EVA. The sample is provided in the form of granular (Fig. S3a). By heating up the sample to 373 K in a furnace, the pellets melt into clear fluid (Fig. S3b) which exhibit high viscosity (Fig. S3c to S3e). The liquid solidifies at ambient temperature (~293 K) (Fig. S3f to S3g). The solid state of the polymer is flexible, which is shown in Figure S3h.

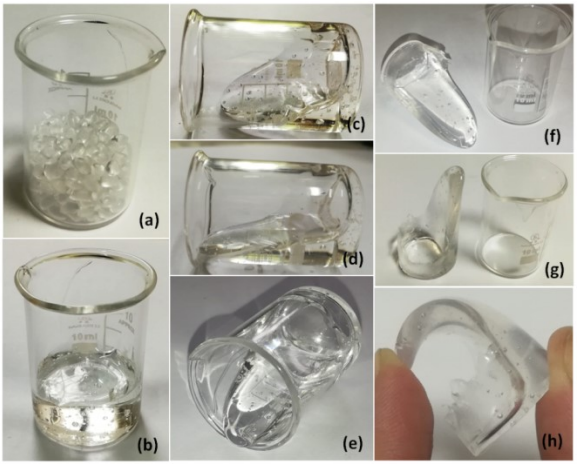

Fig. S3. The viscous liquid and flexible solid states of EVA-18

3. Measurements of V_S and ΔT_{ad}

An electronic universal testing machine (WDW-T50, Tianchen, China) equipped with a temperature-controlled cabinet together with a home-made compression mould was used to record the V_S and ΔT_{ad} changes with the applied pressures.

3.1 Measuring setup of V_S

The compression mould used for the measurements of V_S (Fig. S4) contains: 1) a bottom, 2) a vessel, 3) a driving piston, 4) two copper gaskets, and 5) sample. The copper gaskets are prepared by hot-pressing copper powder under 500 MPa at 373 K for 10 mins using this mould before the measurements. The obtained copper gaskets fit well with the vessel, show good ductility under high pressure, and thereby can seal the samples near the melting points. To ensure the compactness of the pellet-shape sample filled in the mould, the mould is first heated up to above the fusion point of the sample, then a pressure of 10 MPa is applied and kept for at least 15 mins, followed by slowly cooling down to RT. After this treatment, the granular-shape sample becomes a dense cylinder which does not contain any visible bubbles.

The compressibility curves are translated from the relative height-change of the cylinder-shape sample with the variation of pressure. The compressibility of the empty mould, including the bottom, gaskets, and driving piston, is subtracted as a background. The specific volumes V_S are calculated from the height, the diameter (10 mm) and the mass of the cylinder-shape sample. The height of sample under a constant pressure is found to have strong temperature dependence, so V_S is highly temperature-dependent. But the height of the empty mould is nearly independent with temperature, so this influence can be ignored.

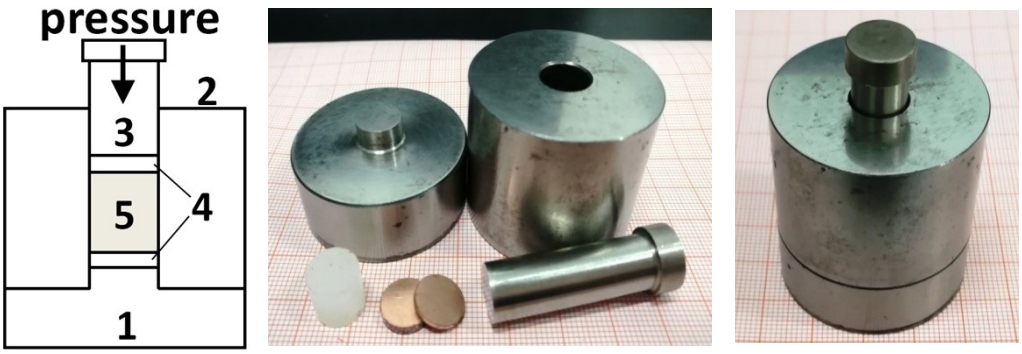

Fig. S4. The compression mould used for the V_S measurements. It contains: 1) a bottom, 2) a vessel, 3) a driving piston, 4) two copper gaskets, and 5) sample.

3.2 V_S-P curves for the PE and EVA-28

The PE and EVA-28 are selected as the representatives to study the compressibility at RT with increasing and decreasing pressure up to 100, 200, 300, and 400 MPa by using the compression mould. The compressibility is defined as the relative volumetric contraction under unit external pressure.[8] A slow rate of 5 MPa/S is used to minimize the variations of sample temperature for a quasi-isothermal condition. The compressibility of EVA-28 (~0.28 GPa^{-1}) found to be larger than that of the PE (~0.20 GPa^{-1}) under 400 MPa, foretelling a giant BCE in it. The hysteresis during compression and decompression processes is attributed to the deformation-driven orthorhombic-monoclinic phase transition in PE.[5] As to the EVA-28, its hysteresis behaviour could be related to the rearrangements of disordered polymer chains with varying pressures.

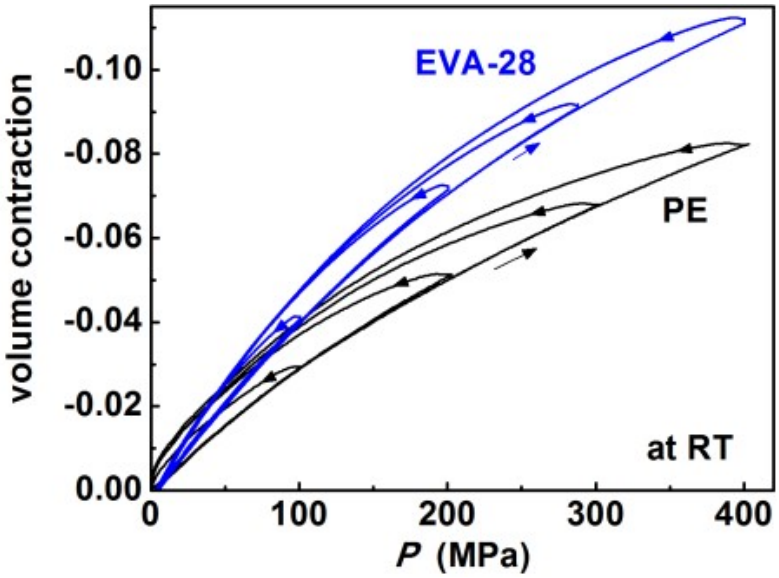

Fig. S5. V_S-P curves for the PE and EVA-28

3.3 Measuring setup of ΔT_{ad} and its validation

According to the references, the ΔT_{ad} can be directly measured by using a compression mould for an elastic polymer, such as the PDMS, nitrile butadiene and nature rubbers.[1,9-12] The compression mould used in this work is very similar with the reported setup.[1,9] The compression mould used for the direct measurements of ΔT_{ad} contains: 1) a bottom, 2) a vessel, 3) a driving piston, 4) a copper gasket, 5) a paper gasket, 6) a T-type thermal couple, and 7) granular-shape sample (Fig. S6). The paper gasket is prepared by pressing a roll of paper tape under 600 MPa at

RT. In order to fix the thermal couple on the mould, there are two small holes drilled on the paper gasket and two notches on the bottom. The probe tip of the thermal couple is covered by the granular-shape sample. The testing points of the ΔT_{ad} measurements are arranged in a cooling sequence from liquid to solid states, which ensures a good thermal contact between the thermal couple and the sample. Both copper and paper gaskets fit well with the vessel, showing good ductility under high pressure, and thereby can seal the sample near the melting points.

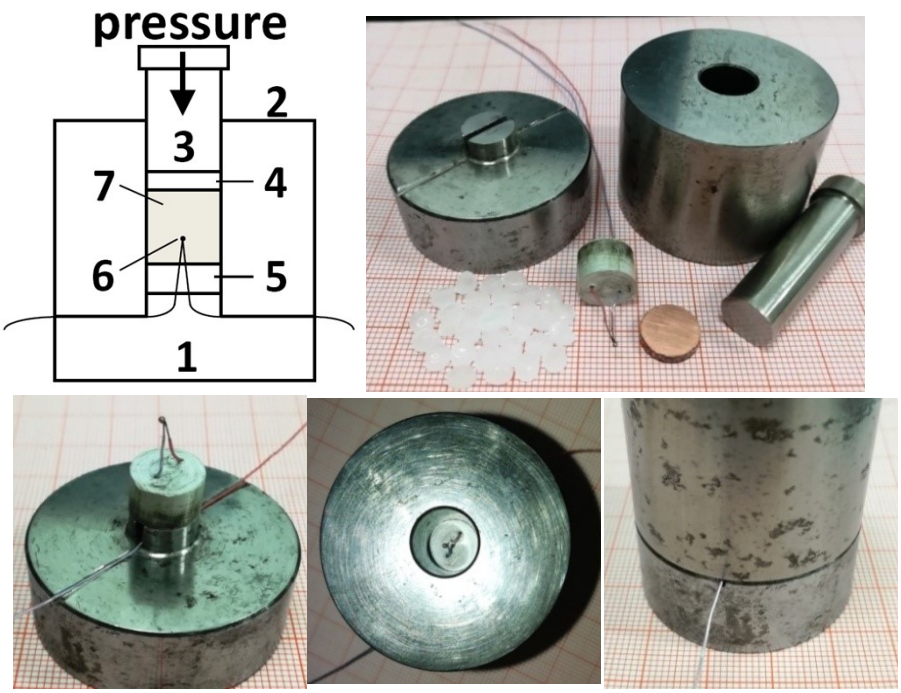

Fig. S6. The compression mould used for the ΔT_{ad} measurements. It contains: 1) a bottom, 2) a vessel, 3) a driving piston, 4) a copper gasket, 5) a paper gasket, 6) a T-type thermal couple, and 7) sample.

We have measured ΔT_{ad} of nitrile butadiene rubber particles and compared our results with the reported values to check validity of our home-made setup. Pressures of 100, 150, 200, 250, 300, 350, and 400 MPa are applied and removed rapidly to measure the positive and negative ΔT_{ad} around 303 K (Fig. S7). Taking it into account that the differences in the thermal conductivity of chamber and the speeds of compression and decompression exist inevitably, our testing results basically agree with the values which are estimated from the figure in Reference 1 (Fig. S8). Therefore, the obtained giant ΔT_{ad} values by using this home-made measuring setup are reliable.

However, there are comparatively larger discrepancies of $|\Delta T_{ad}|$ during compressions and decompressions in our testing results. The possible reasons are discussed below. As is mentioned above, the copper gaskets fit well with the vessel and seal the liquid well under high pressure. The frictional heating between the gasket and chamber wall would enhance the temperature rises during compression but reduce the temperature drops during decompression. In a practical cooling device, the leakage problem of a liquid can be solved by enclosing it into small elastic capsules, instead of by using the frictional gaskets. Besides, the nitrile butadiene rubber particles are highly elastic. The interstitial spaces among the particles emerge during decompression, which can reduce the heat transfer between the sample and thermal couple, and thereby, the detected temperature drops.

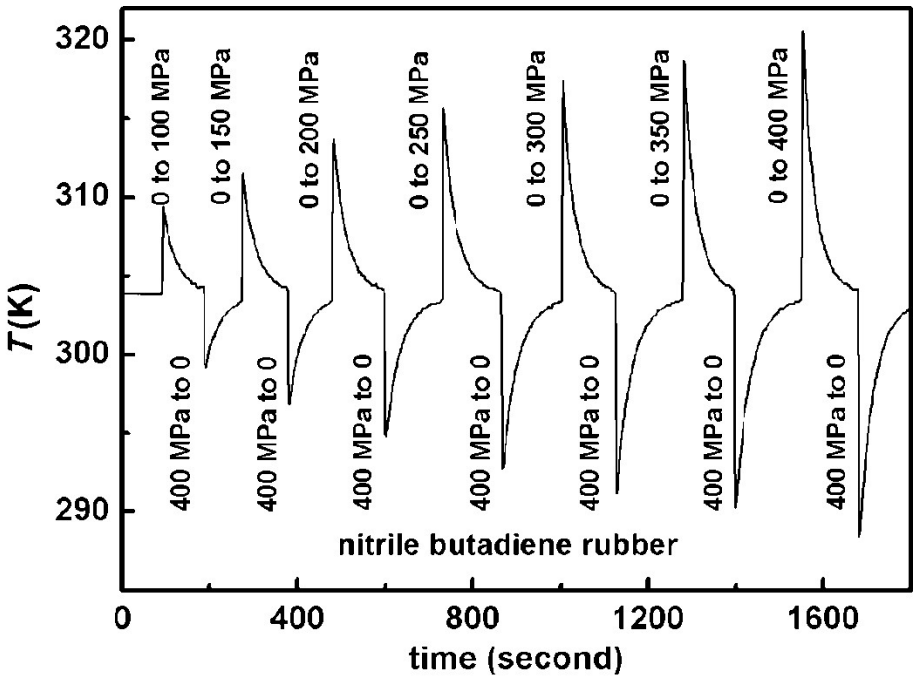

Fig. S7. Sample temperature versus time under rapid compressions and decompressions for the nitrile butadiene rubber particles.

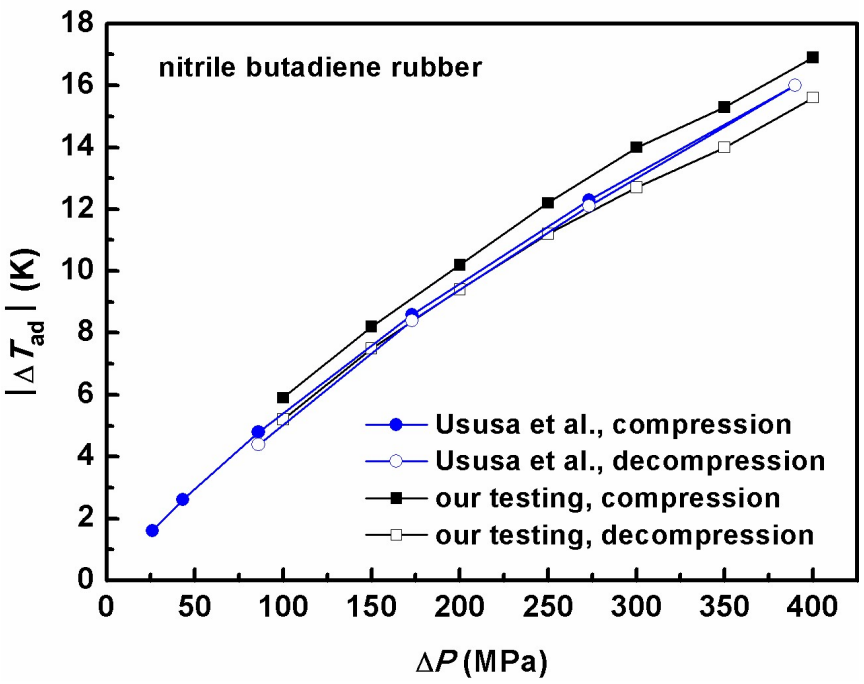

Fig. S8. Comparison of $|\Delta T_{ad}|$ between the values measured by us and the values reported by Ususa et al for the nitrile butadiene rubber.

We have measured ΔT_{ad} of NaCl powder by using this compression mould and obtained a value of about 4.4/-3.4 K under the compression/decompression of 400 MPa around 298 K which is shown in the following figure. This value is much lower than the prediction of 6.9 K from a fitting curve proposed by Boehler:$^{(\partial T/\partial P)_S = 1.90 - 0.0467P + 0.0008440P^2 - 0.000008006P^3}$, which describes the adiabatic pressure (in kilobars) derivative of temperature of NaCl at 298 K.[13] This deviation can be understood in the following points. On the one hand, the ductility and elasticity of NaCl is much lower than the polymer. The uniaxial pressure of 400 MPa is not high enough to compact the NaCl powder and to transmit the pressure uniformly without a pressure-transmitting medium. On the other hand, the very sharper spikes on the temperature-time curves make it difficult to capture the peak values due to the relatively low sampling rate of 1 point/second in our measurement. These very sharper spikes could be related to the higher thermal conductivity of NaCl compared with the polymers which leads to the rapid temperature recovery after the compressions and decompressions.

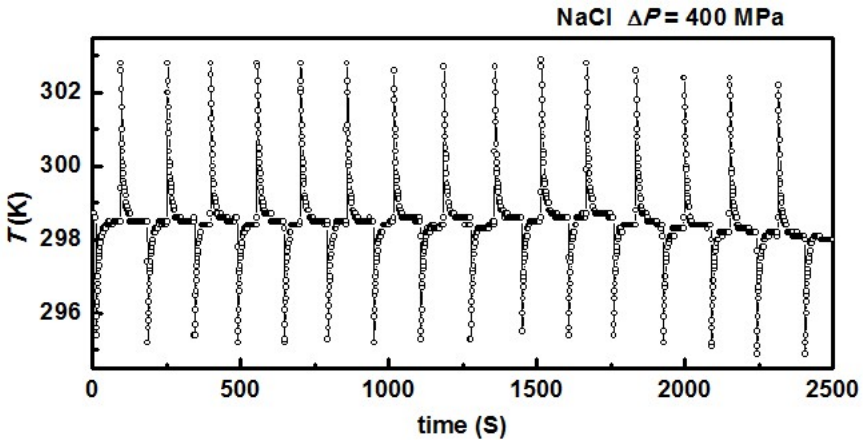

Fig. S9. Sample temperature versus time under rapid compressions and decompressions of 400 MPa for the NaCl particles.

In summary, the barocaloric effects of an elastic/plastic solid or a viscous liquid can be investigated by using a uniaxial compression mould without a pressure-transmitting medium. As to a material with relatively high compressive modulus, there would have a large underestimation of ΔT_{ad} because the hydrostatic condition may not be well satisfied. As for a material with high thermal conductivity, a high-speed temperature recorder is required for capturing the very sharp spikes of ΔT_{ad}.

3.4 ΔT_{ad}-T curves for the PE and EVAs

The ΔT_{ad}-T curves measured under rapid compressions and decompressions of 100, 200, 300 and 400 MPa for the PE, EVA-18, EVA-28 and EVA-40 are shown here (Fig. S9 to S12) The typical procedure of the ΔT_{ad} measurement is introduced in Fig. 2. The testing points of the ΔT_{ad} measurements are arranged in a cooling sequence from liquid to solid states.

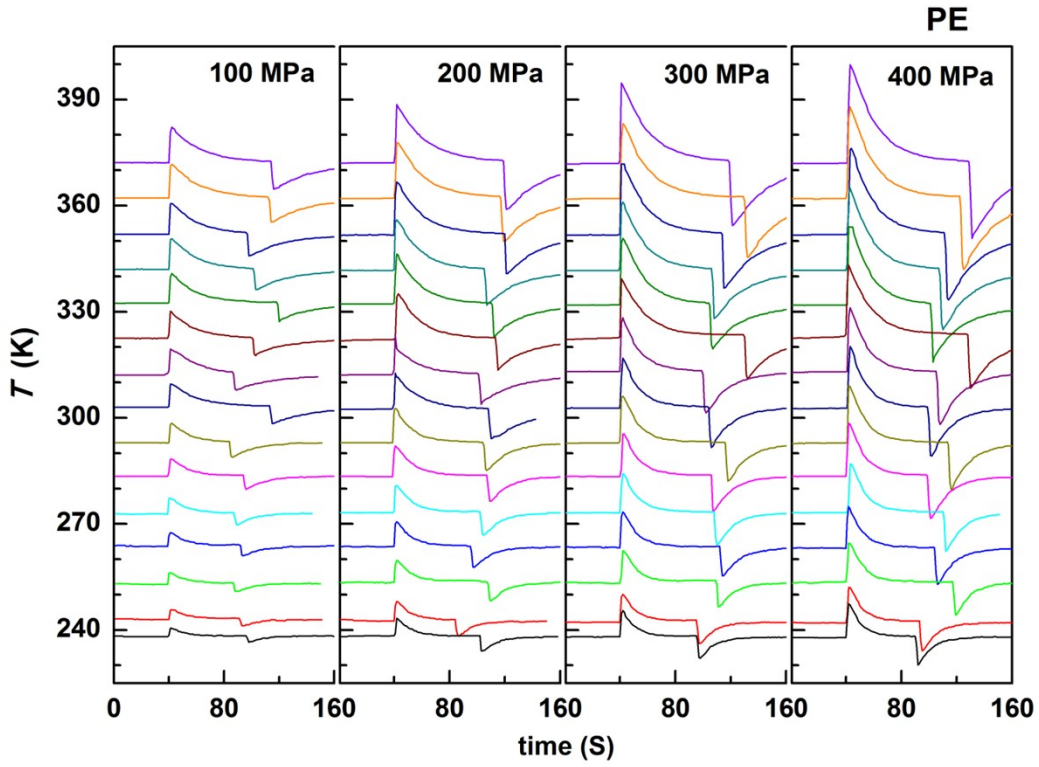

Fig. S10. The ΔT_{ad}-T curves for the PE.

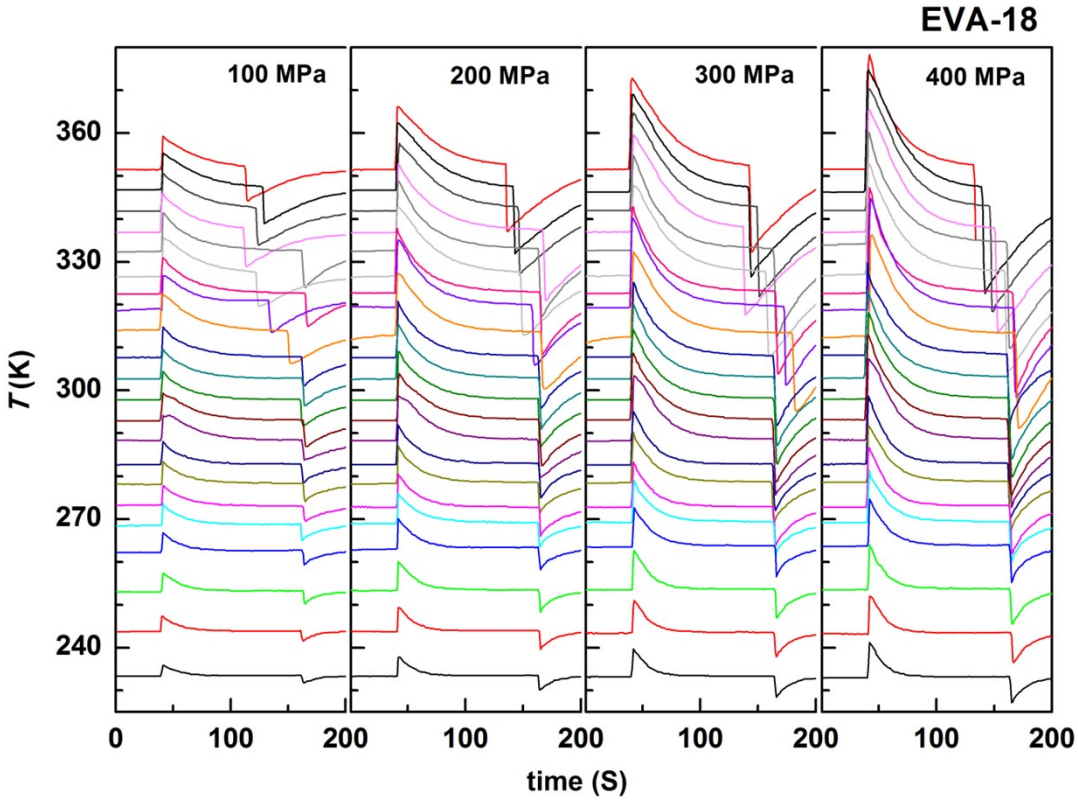

Fig. S11. The ΔT_{ad}-T curves for the EVA-18.

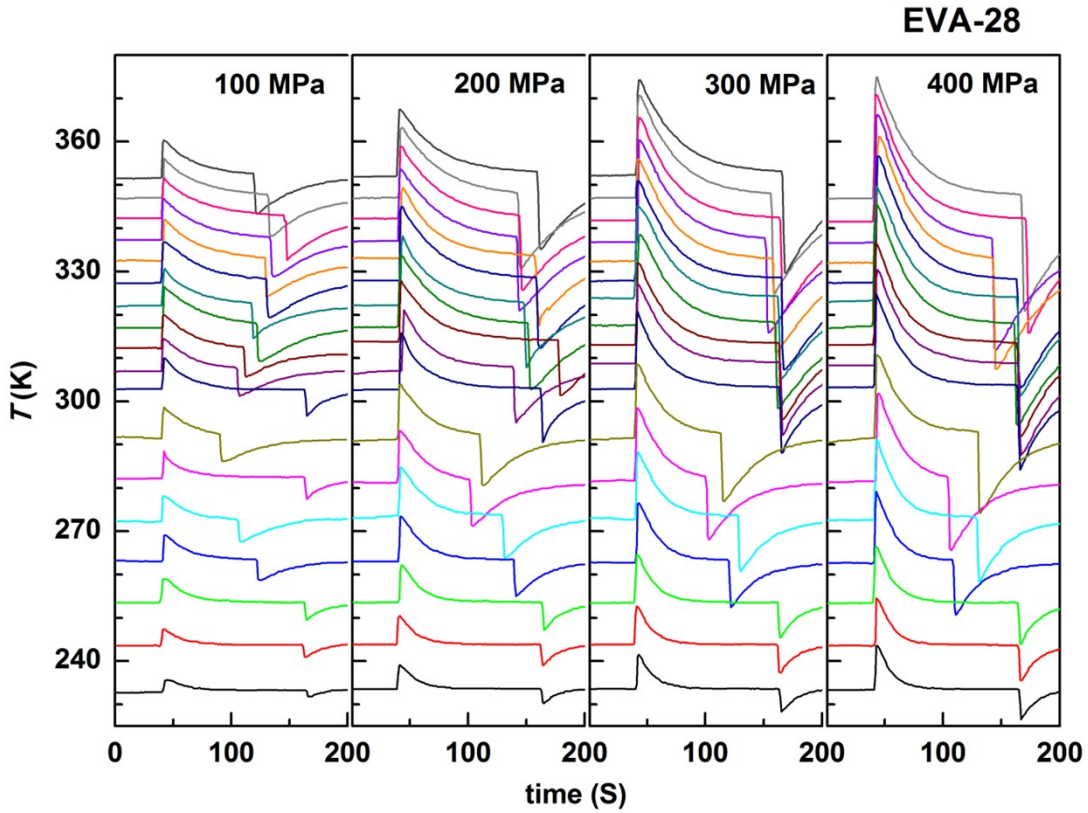

Fig. S12. The ΔT_{ad}-T curves for the EVA-28.

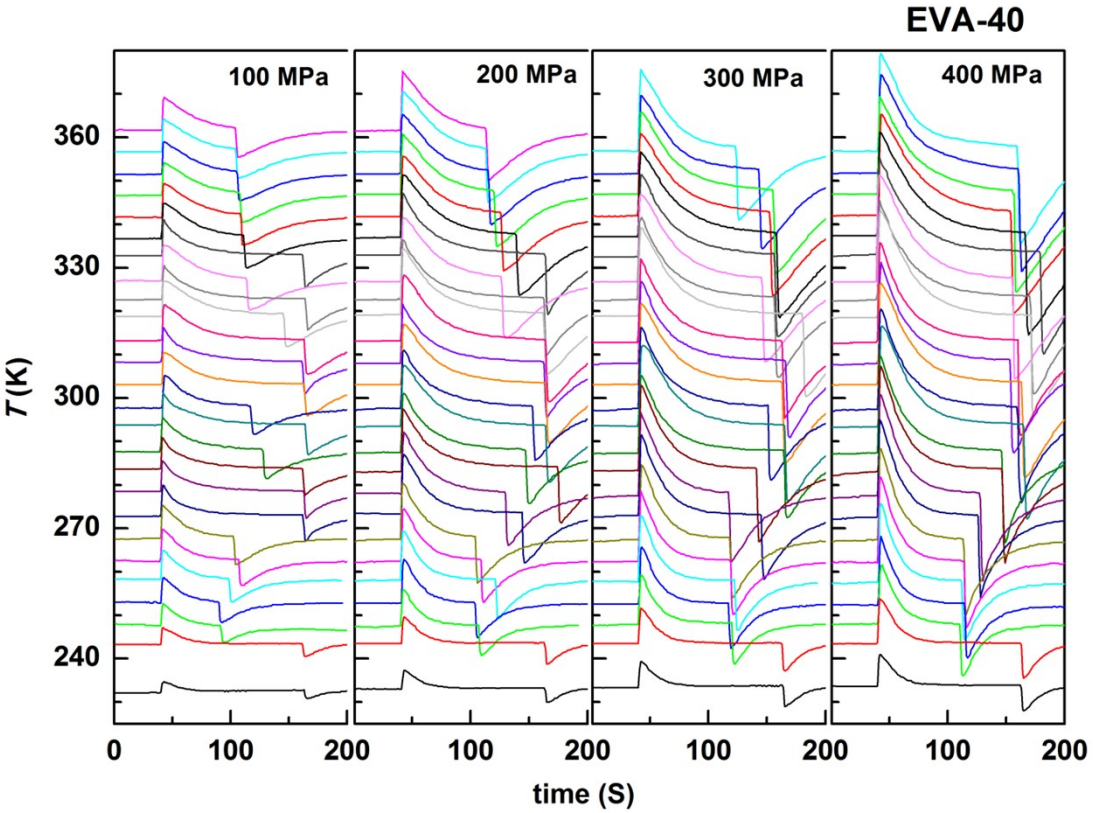

Fig. S13. The ΔT_{ad}-T curves for the EVA-40.

4. References

1 E. O. Usuda, W. Imamura, N. M. Bom, L. S. Paixão, A. M. G. Carvalho, Giant Reversible Barocaloric Effects in Nitrile Butadiene Rubber around Room Temperature. ACS Appl. Polym. Mater., 2019, **1**, 1991-1997.

2 A. Albrecht, R. Brüll, T. Macko, F. Malz, H. Pasch, Comparison of high-temperature HPLC, CRYSTAF and TREF for the analysis of the chemical composition distribution of ethylene-vinyl acetate copolymers. Macromol. Chem. Phys., 2009, **210**, 1319-1330.

3 M. Çopuroğlu, M. Şen, A comparative study of thermal ageing characteristics of poly(ethylene-co-vinyl acetate) and poly(ethylene-co-vinyl acetate)/carbon black mixture. Polym. Adv. Technol., 2004, **15**, 393-399.

4 D. A. Silva, H. R. Roman, P. J. P. Gleize, Evidences of chemical interaction between EVA and hydrating Portland cement, Cement and Concrete Res., 2002, **32**, 1383-1390.

5 R. Wang, S. L. Fang, Y. C. Xiao, E. L Gao, N. Jiang, Y. W. Li, L. L. Mou, Y. A. Shen, W. B. Zhao, S. T. Li, A. F. Fonseca, D. S. Galvão, M. M. Chen, W. Q. He, K. Q. Yu, H. B. Lu, X. M. Wang, D. Qian, A. E. Aliev, N. Li, C. S. Haines, Z. S. Liu, J. K. Mu, Z. Wang, S. G. Yin, M. D. Lima, B. G. An, X. Zhou, Z.F. Liu, R. H. Baughman, Torsional refrigeration by twisted, coiled, and supercoiled fibers. Science, 2019, **366**, 216-221.

6 A. Albrecht, R. Brüll, T. Macko, F. Malz, H. Pasch, Comparison of high-temperature HPLC, CRYSTAF and TREF for the analysis of the chemical composition distribution of ethylene-vinyl acetate copolymers. Macromol. Chem. Phys., 2009, **210**, 1319-1330.

7 M. Sadeghi, G. Khanbabaei, A. H. S. Dehaghani, M. Sadeghi, M. A. Aravand, M. Akbarzade, S. Khatti, Gas permeation properties of ethylene vinyl acetate-silica nano composite membranes. J. Membrane Sci., 2008, **322**, 423-428.

8 B. Li, Y. Kawakita, S. Ohira-Kawamura, T. Sugahara, H. Wang, J. F. Wang, Y. N. Chen, S. I. Kawaguchi, S. Kawaguchi, K. Ohara, K. Li, D. H. Yu, R. Mole, T. Hattori, T. Kikuchi, S. I. Yano, Z. Zhang, Z. Zhang, W. J. Ren, S. C. Lin, O. Sakata, K. Nakajima, Z. D. Zhang, Colossal barocaloric effects in plastic crystals. Nature , 2019, **567**, 506.

9 N. M. Bom, E. O. Usuda, G. M. Guimarães, A. A. Coelho, A. M. G. Carvalho, Experimental setup for measuring the barocaloric effect in polymers: Application to natural rubber, Rev. Sci. Instrum., 2017, **88**, 046103.

10 E. O. Usuda, N. M. Bom, A. M. G. Carvalho, Large barocaloric effects at low pressures in natural rubber. Eur. Polym. J., 2017, **92**, 287-293.

11 N. M. Bom, W. Imamura, E. O. Usuda, L. S. Paixão, A. M. G. Carvalho, Giant Barocaloric Effects in Natural Rubber: A Relevant Step toward Solid-State Cooling. ACS Macro Lett., 2018, **7**, 31-36.

12 A. M. G. Carvalho, W. Imamura, E. O. Usuda, N. M. Bom, Giant Room-Temperature Barocaloric Effects in PDMS Rubber at Low Pressures. Eur. Polym. J., 2018, **99**, 212-221.

13 R. Boehler, Adiabats $(\partial T/\partial P)_S$ and Grüneisen parameter of NaCl up to 50 kilobars and 800°C. J. Geophys. Res., 1981, **86**, 7159-7162,